New Test Beam Results of 3D and Pad Detectors Constructed with Poly-Crystalline CVD Diamond

M. Reichmann[z,*], A. Alexopoulos[c], M. Artuso[t], F. Bachmair[x], L. Bäni[x], M. Bartosik[c], J. Beacham[m], H. Beck[w], V. Bellini[b], V. Belyaev[l], B. Bentele[s], P. Bergonzo[k], A. Bes[aa], J-M. Brom[g], M. Bruzzi[d], G. Chiodini[z], D. Chren[r], V. Cindro[i], G. Claus[g], J. Collot[aa], J. Cumalat[s], A. Dabrowski[c], R. D'Alessandro[d], D. Dauvergne[aa], W. de Boer[j], S. Dick[m], C. Dorfer[x], M. Dünser[c], G. Eigen[ad], V. Eremin[f], J. Forneris[o], L. Gallin-Martel[aa], M.L. Gallin-Martel[aa], K.K. Gan[m], M. Gastal[c], C. Giroletti[q], M. Goffe[g], J. Goldstein[q], A. Golubev[h], A. Gorišek[i], E. Grigoriev[h], J. Grosse-Knetter[w], A. Grummer[u], M. Guthoff[c], B. Hiti[i], D. Hits[x], M. Hoeferkamp[u], T. Hofmann[c], J. Hosslet[g], J-Y. Hostachy[aa], F. Hügging[a], C. Hutton[q], J. Janssen[a], H. Kagan[m], K. Kanxheri[ab], R. Kass[m], M. Kis[e], G. Kramberger[i], S. Kuleshov[h], A. Lacoste[aa], S. Lagomarsino[d], A. Lo Giudice[o], E. Lukosi[y], C. Maazouzi[g], I. Mandic[i], A. Marino[s], C. Mathieu[g], M. Menichelli[ab], M. Mikuž[i], A. Morozzi[ab], J. Moss[ac], R. Mountain[t], S. Murphy[v], M. Muškinja[i], A. Oh[v], P. Oliviero[o], D. Passeri[ab], H. Pernegger[c], R. Perrino[z], F. Picollo[o], M. Pomorski[k], R. Potenza[b], A. Quadt[w], F. Rarbi[aa], A. Re[o], G. Riley[ab], S. Roe[c], D.A. Sanz-Becerra[x], M. Scaringella[d], D. Schaefer[c], C.J. Schmidt[e], E. Schioppa[c], S. Schnetzer[n], S. Sciortino[d], A. Scorzoni[ab], S. Seidel[u], L. Servoli[ab], D.S. Smith[m], B. Sopko[r], V. Sopko[r], S. Spagnolo[z], S. Spanier[y], K. Stenson[s], R. Stone[n], B. Stugo[ad], C. Sutera[b], M. Traeger[e], D. Tromson[k], W. Trischuk[p], C. Tuve[b], J. Velthuis[q], N. Venturi[c], E. Vittone[o], S. Wagner[s], R. Wallny[x], J.C. Wang[t], C. Weiss[c], N. Wermes[a], M. Yamouni[aa], M. Zalieckas[ad], M. Zavrtanik[i]

[a]Universität Bonn, Bonn, Germany, [b]INFN/University of Catania, Catania, Italy, [c]CERN, Geneva, Switzerland, [d]INFN/University of Florence, Florence, Italy, [e]GSI, Darmstadt, Germany, [f]Ioffe Institute, St. Petersburg, Russia, [g]IPHC, Strasbourg, France, [h]ITEP, Moscow, Russia, [i]Jožef Stefan Institute, Ljubljana, Slovenia, [j]Universität Karlsruhe, Karlsruhe, Germany, [k]CEA-LIST Technologies Avancees, Saclay, France, [l]MEPHI Institute, Moscow, Russia, [m]The Ohio State University, Columbus, OH, USA, [n]Rutgers University, Piscataway, NJ, USA, [o]University of Torino, Torino, Italy, [p]University of Toronto, Toronto, ON, Canada, [q]University of Bristol, Bristol, UK, [r]Czech Technical University, Prague, Czech Republic, [s]University of Colorado, Boulder, CO, USA, [t]Syracuse University, Syracuse, NY, USA, [u]University of New Mexico, Albuquerque, NM, USA, [v]University of Manchester, Manchester, UK, [w]Universität Göttingen, Göttingen, Germany, [x]ETH Zürich, Zürich, Switzerland, [y]University of Tennessee, Knoxville, TN, USA, [z]INFN-Lecce, Lecce, Italy, [aa]LPSC-Grenoble, Grenoble, France, [ab]INFN-Perugia, Perugia, Italy, [ac]California State University, Sacramento, CA, USA, [ad]University of Bergen, Bergen, Norway,

[*]Corresponding author

Abstract

The RD42 collaboration is investigating Chemical Vapour Deposition (CVD) diamond as a future material for particle detectors in a harsh radiation environment. The latest beam test results of 3D pixel detectors fabricated with poly-crystalline CVD (pCVD) diamonds will be shown. The cells of the devices have a size of $50\,\mu\mathrm{m} \times 50\,\mu\mathrm{m}$ with columns $2.6\,\mu\mathrm{m}$ in diameter. In one of the devices the cells were ganged in a 3×2 cell and in the other in a 1×5 pattern to match the layouts of the pixel read-out chips currently used in the CMS and ATLAS experiments at the LHC, respectively. In beam tests, using tracks reconstructed with a high precision tracking telescope, both devices achieved tracking efficiencies greater than 97 %. These efficiencies were already achieved at bias voltages greater than 30 V.

Finally, the latest high rate beam test results of irradiated pCVD diamond pad detectors will be discussed. In many measurements with with particle fluxes up to $20\,\mathrm{MHz/cm^2}$ and irradiations up to $4 \cdot 10^{15}\,\mathrm{n/cm^2}$ it could be shown that irradiated pCVD diamonds are not depending on the rate to the $\mathcal{O}\,(2\,\%)$.

Keywords: Diamond Detectors, 3D, Rate

1. Introduction

Motivation. The radiation damage created by the High-Luminosity-LHC (HL-LHC) will become a big challenge for the detector. By 2028 an instantaneous luminosity of $5 \cdot 10^{34}\,\mathrm{cm^{-2}\,s^{-1}}$ is expected [1]. In this environment the innermost tracking layer at a distance of ~30 mm to the interaction point (IP) is expected to be exposed to a total fluence of $2 \cdot 10^{16}\,\mathrm{n_{eq}/cm^2}$ by this time [2].

After large irradiation, all detector materials become trap limited with a mean drift distance (MDD) below $75\,\mu\mathrm{m}$. Due to its great properties, such as the large displacement energy of 42 eV/atom and the high band gap of 5.5 eV, the RD42 collaboration is investigating CVD diamond possible candidate. In various studies it was shown that compared to corresponding silicon detectors, diamond is at minimum three times more radiation hard [3], has at least a two times faster charge collection [4] and its thermal conductivity is four times higher [5].

Introduction. By now the technology of diamond detectors is well established in high energy physics. Many of the experiments are already using Beam Condition Monitors (BCMs) or Beam Loss Monitors (BLMs) based on CVD diamonds.

The RD42 collaboration is also investigating a novel detector design, namely 3D detectors. This concept is a possible way to reduce the drift distance below a critical MDD without reducing the total number of the created electron-hole pairs. Since the particle flux of the HL-LHC will be in completely new regime, high rate studies of pad detectors are performed at Paul Scherrer Institut (PSI) with nearly minimum ionising particles (MIPs) and tunable particle fluxes up to $\mathcal{O}\left(10\,\mathrm{MHz/cm^2}\right)$.

2. 3D Pixel Detectors

3D detectors can largely reduce the drift distance of the charge carriers induced by ionising particles. More details about the working principle can be found in [6], [7].

Fabrication. In order to generate these electrodes in diamond the columns are drilled with a 800 nm femtosecond laser which converts the diamond into a resistive mixture of different carbon phases [8]. By using Spacial Light Modulation (SLM) a column yield of >99 % and a column diameter of 2.6 µm can be achieved [9]. The largest fabricated device has about 4000 of these cells.

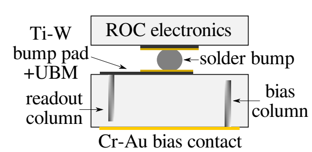

Figure 1: Bump bonding scheme.

The final detector is then built by connecting to the bias and readout columns with surface metallisation and bump bonding the sensor to the readout electronics as shown in Figure 1. For the latest detectors a cell size of $50\,\mu\mathrm{m} \times 50\,\mu\mathrm{m}$ was chosen. Since the layout of the available readout chips (ROCs) has a different pixel pitch several cells had to be ganged together.

PSI46digV2.1respin. The first prototype of a 50 µm × 50 µm 3D pixel detector is connected to the CMS PSI46digV2.1respin ROC [11] with a 3 × 2 ganging to

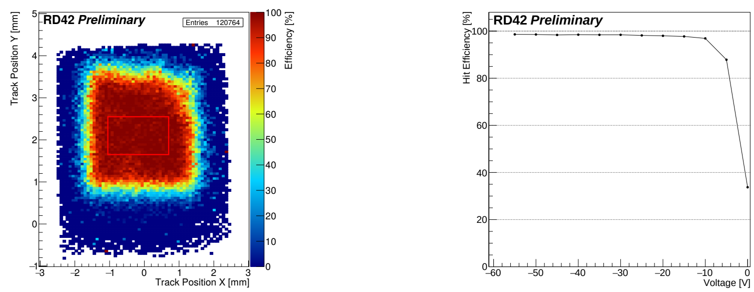

(a) 3 × 2 efficiency.

(b) Efficiency vs. voltage.

Figure 2: 3 × 2 results.

match the pixel pitch of 150 µm × 100 µm. In this case indium bump are used to connect to the ROC. The preliminary beam test results show an efficiency of 99.2 % (Figure 2a). This value is close to the efficiency of a silicon pixel of 99.9 % which was tested in parallel. Compared to the silicon the 3D pixel detector has a relative efficiency of 99.3 %. For this value it was not considered that some of the 3D cells are not working. Due to the bad tracking resolution at PSI it is not possible to detect them in this measurement. Nevertheless a small mismatch is expected due to low field regions between the electrodes and the columns themselves. Figure 2b shows the the device is already fully efficient at a Voltage of 30 V and stays constant for higher voltages.

The measured pulse height of ∼11 ke is consistent with the measurement in the next paragraph due to the different momentum of the incident particles.

FE-I4. The second prototype is connected to the ATLAS FE-I4 ROC [10] with a 1 × 5 ganging due to its pitch of 50 µm × 250 µm . The bump bonding was done using a adapted process with tin-silver bumps. Using a beam telescope with 3 µm spatial resolution the efficiency could could be mapped to the spatial coordinates yielding an efficiency of 97.8 % over a contiguous area (Figure 3). However there are many small regions where the device is almost completely inefficient.

The reason for this are most likely issues with the bump bonding or the metallisation. Nevertheless the preliminary pulse height in the good region already amount to $\sim$15 ke which corresponds to a charge collection efficiency (CCE) of more than 80 %.

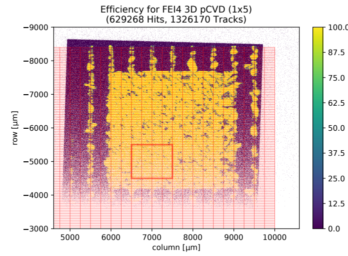

Figure 3: 1×5 efficiency

3. High Rate Studies

Since the HL-LHC will reach particle fluxes of $\mathcal{O}\left(\mathrm{GHz/cm^2}\right)$ it is very important to understand the effect of the incident particle flux on the signal of pCVD diamonds.

Test Site. In order to conduct such a study it is essential to be able to vary the particle flux over a large range. The πM1 beam line at the High Intensity Proton Accelerator (HIPA) at PSI [12] can provide beams with continuously tunable fluxes from the order of 1 kHz/cm^2 up to 20 MHz/cm^2. It is a bunched beam with a spacing of 19.7 ns. For these studies a π^+ beam with with a momentum of 260 MeV/c was chosen in order to reach the highest possible flux [13].

Setup. The diamond sensors were connected in a pad geometry and prepared as described in [14]. In order to resolve single waveforms at high particle rates the sensors were connected to a fast, low-noise amplifier with a rise time of approximately 5 ns. The resulting waveforms are then digitised and recorded in a beam telescope setup which provides spatial information of the hits in the diamond detector.

Results. pCVD diamond has a interior crystal structure where the single grains have slightly different properties. Due to that the size of the measured signal in pCVD depends also on the spatial position as can be seen in Figure 4. However this behaviour is constant and does not depend on time or rate.

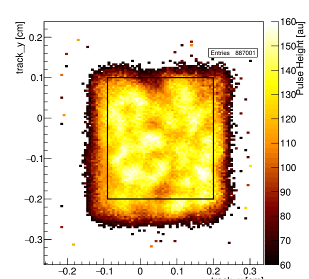

Figure 4: Signal map of a pCVD detector.

As an important factor also the leakage current is studied depending on the particle rate. In 80 % of the measured diamonds the current is proportional and the base current without beam is of the $\mathcal{O}\,(1\,\mathrm{nA})$. Some bad diamonds show shifting base lines or even erratic currents [15].

In order to measure the signal behaviour depending on the incident particle flux several rate scans with both polarities of the bias voltage and different irradiation doses were performed. Figure 5 shows the final results for a pCVD diamond with various irradiations with reactor neutrons up to $8 \cdot 10^{15}\,\mathrm{n/cm^2}$. An upper limit of the pulse height dependence on particle flux for irradiated devices of less than 2 % was observed for a flux up to $20\,\mathrm{MHz/cm^2}$. But we also observed a single diamond that showed a very strong rate dependence of more than 90 %. However, after the sensor was cleaned with Reactive Ion Etching (RIE) and fully reprocessed a new measurement showed a dependence of less than 2 %. This lead us to the conclusion that these effects result from surface contamination and it is possible to repair them.

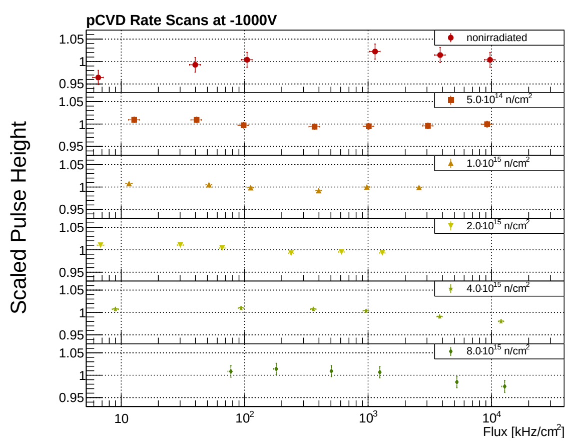

Figure 5: Pulse height versus incident particle flux for a pCVD diamond for different irradiations

After the irradiation the pulse height decreases due to the radiation damage.

There was no absolute calibration done yet which is required to relate the pulse height values before and after irradiation.

4. Conclusion

There is great progress in the development of more radiation tolerant particle detectors based on pCVD diamonds. The working principle of 3D pixel detectors was proven with great success down to cell sizes of $50\,\mu\text{m} \times 50\,\mu\text{m}$ and column diameters of $2.6\,\mu\text{m}$. The number of cells could be scaled up by a factor of 40 to 4000. For the first time more than 80 % of the created charge in the material was read out. The efficiency of the column drilling process is now above 99 % and the relative efficiency of the 3D pixel detectors is 99.3 % compared to a silicon device.

In extensive studies it was found that irradiated pCVD diamond detectors work reliably and show no signal dependence to the $\mathcal{O}(2\,\%)$ up to an incident particle flux of $20\,\text{MHz/cm}^2$. This was shown for an irradiation up to a fluence of $8 \cdot 10^{15}\,\text{n/cm}^2$. The leakage current of a good detector is proportional to the flux and of the $\mathcal{O}(1\,\text{nA})$ without beam. Some diamonds show a strong rate dependence which is most likely to surface contamination and is possible to overcome.

List of Acronyms

ROC readout chip

HL-LHC High-Luminosity-LHC

PSI Paul Scherrer Institut

HIPA High Intensity Proton Accelerator

MIP minimum ionising particle

CVD Chemical Vapour Deposition

pCVD poly-crystalline CVD

BCM Beam Condition Monitor

BLM Beam Loss Monitor

IP interaction point

CCE charge collection efficiency

MDD mean drift distance

SLM Spacial Light Modulation

RIE Reactive Ion Etching

References

[1] G. Apollinari, I. Béjar Alonso, O. Brüning, M. Lamont, L. Rossi, High-Luminosity Large Hadron Collider (HL-LHC): Preliminary Design Report, CERN Yellow Reports: Monographs, CERN, Geneva, 2015.
URL https://cds.cern.ch/record/2116337

[2] G. Auzinger, Upgrade of the CMS Tracker for the High Luminosity LHC, Tech. Rep. CMS-CR-2016-268, CERN, Geneva (Oct 2016).
URL https://cds.cern.ch/record/2227193

[3] W. de Boer, J. Bol, A. Furgeri, S. Müller, C. Sander, E. Berdermann, M. Pomorski, M. Huhtinen, Radiation hardness of diamond and silicon sensors compared, physica status solidi (a) 204 (9) (2007) 3004–3010. doi:10.1002/pssa.200776327.
URL http://dx.doi.org/10.1002/pssa.200776327

[4] H. Pernegger, V. Eremin, H. Frais-Kölbl, E. Griesmayer, H. Kagan, S. Roe, S. Schnetzer, R. Stone, W. Trischuk, D. Twitchen, P. Weilhammer, A. Whitehead, Charge-carrier properties in synthetic single-crystal diamond measured with the transient-current technique, J. Appl. Phys.

97 (7) (2005) 73704–1–9.
URL https://cds.cern.ch/record/909063

[5] S. Zhao, Characterization of the electrical properties of polycrystalline diamond films, Ph.D. thesis, The Ohio State University (1994).
URL http://wwwlib.umi.com/dissertations/fullcit?p9421043

[6] F. Bachmair, L. Bäni, P. Bergonzo, B. Caylar, G. Forcolin, I. Haughton, D. Hits, H. Kagan, R. Kass, L. Li, A. Oh, S. Phan, M. Pomorski, D. Smith, V. Tyzhnevyi, R. Wallny, D. Whitehead, A 3D diamond detector for particle tracking, Nuclear Instruments and Methods in Physics Research Section A: Accelerators, Spectrometers, Detectors and Associated Equipment 786 (2015) 97 – 104. doi:https://doi.org/10.1016/j.nima.2015.03.033.
URL http://www.sciencedirect.com/science/article/pii/S0168900215003496

[7] S. Parker, C. Kenney, J. Segal, 3D - A proposed new architecture for solid-state radiation detectors, Nuclear Instruments and Methods in Physics Research Section A: Accelerators, Spectrometers, Detectors and Associated Equipment 395 (3) (1997) 328 – 343, proceedings of the Third International Workshop on Semiconductor Pixel Detectors for Particles and X-rays. doi:https://doi.org/10.1016/S0168-9002(97)00694-3.
URL http://www.sciencedirect.com/science/article/pii/S0168900297006943

[8] T. Kononenko, M. Komlenok, V. Pashinin, S. Pimenov, V. Konov, M. Neff, V. Romano, W. Lüthy, Femtosecond laser microstructuring in the bulk of diamond, Diamond and Related Materials 18 (2) (2009) 196 – 199, nDNC 2008 Proceedings of the International Conference on New Diamond and Nano Carbons 2008. doi:https://doi.org/10.1016/j.diamond.2008.07.014.
URL http://www.sciencedirect.com/science/article/pii/S0925963508003981

[9] B. Sun, P. S. Salter, M. J. Booth, High conductivity micro-wires in diamond following arbitrary paths, Applied Physics Letters 105 (23) (2014) 231105. arXiv:https://doi.org/10.1063/1.4902998, doi:10.1063/1.4902998. URL https://doi.org/10.1063/1.4902998

[10] M. Garcia-Sciveres, D. Arutinov, M. Barbero, R. Beccherle, S. Dube, D. Elledge, J. Fleury, D. Fougeron, F. Gensolen, D. Gnani, V. Gromov, T. Hemperek, M. Karagounis, R. Kluit, A. Kruth, A. Mekkaoui, M. Menouni, J. Schipper, The FE-I4 Pixel Readout Integrated Circuit, Tech. Rep. ATL-UPGRADE-PROC-2010-001, CERN, Geneva (Jan 2010). URL https://cds.cern.ch/record/1231359

[11] A. Kornmayer, T. Müller, U. Husemann, Studies on the response behaviour of pixel detector prototypes at high collision rates for the CMS experiment, presented 04 Dec 2015 (Nov 2015). URL https://cds.cern.ch/record/2264667

[12] High Intesity Proton Accelerator at PSI, https://www.psi.ch/rf/hipa (2017).

[13] Pion and electron fluxes in piM1, http://aea.web.psi.ch/beam2lines/pim1c.html (2015).

[14] R. Wallny, et al., Beam test results of the dependence of signal size on incident particle flux in diamond pixel and pad detectors, JINST 10 (07) (2015) C07009. URL https://cds.cern.ch/record/2159123

[15] M. Mikuz, V. Cindro, I. Dolenc, H. Kagan, G. Kramberger, H. Frais-Kolbl, A. Gorisek, E. Griesmayer, B. Macek, I. Mandic, M. Niegl, H. Pernegger, D. Smith, D. Tardif, W. Trischuk, P. Weilhammer, M. Zavrtanik, The atlas beam conditions monitor, Vol. 3, 2008, pp. 1914 – 1917. doi:10.1109/NSSMIC.2007.4436530.